https://doi.org/10.46335/IJIES.2026.11.3.2 **e-ISSN: 2456-3463**
Vol. 11, No. 3, 2026, PP. 5-11

International Journal of Innovations in Engineering and Science, www.ijies.net

Sensorless Open-Loop Speed and Torque Control of BLDC Motor

Girish Chandu Dhawak [1], Prashil Siddharth Sukhdeve [2], Aditya Abhimanyu Gawai[3], Mohit Gajanan Bawankar [4], Dr. Sachin Jolhe[5]

[1-5] Electrical Engineering. Dept., Government College of Engineering, Nagpur, Maharashtra, India

girishchandrakantdhawak454@gmail.com

***Received on**: 09 March, 2026* ***Revised on**: 06 April, 2026* ***Published on**: 08 April, 2026*

Abstract*—This paper presents a cost-effective, sensorless, open-loop speed and torque control architecture for a three-phase Brushless DC (BLDC) motor driven by the PIC18F25K22 8-bit microcontroller. Unlike conventional BLDC drive systems that rely on Hall-effect sensors or back-EMF zero-crossing detection, the proposed design achieves phase commutation solely through time-based PWM sequencing generated by the on-chip CCP modules. The high-side/low-side gate driver pair IR2102 controls IRFZ540 power MOSFETs rated at 100 V / 28 A, providing robust switching for each motor phase. A 16x2 LCD connected in 4-bit mode on PORTB displays real-time PWM duty cycle and estimated rotor speed, enabling operator monitoring without external instrumentation. The complete system is verified through Proteus simulation. Comparative analysis demonstrates that the proposed design achieves equivalent steady-state speed regulation under light-load conditions to sensor-based implementations, while reducing system BOM cost by eliminating Hall sensors and their associated signal-conditioning circuitry. The architecture is reproducible, pedagogically transparent, and constitutes a practical foundation for future closed-loop upgrades.*

Keywords—BLDC motor, PIC18F25K22, sensorless control, PWM commutation, IR2102, IRFZ540, open-loop control, LCD monitoring, motor drive, embedded systems.

INTRODUCTION

Because of their higher power density, greater efficiency, and lower maintenance requirements than brushed machines, brushless DC motors have become the preferred actuator in applications ranging from robotics and UAVs to HVAC systems and electric vehicles [1]. The removal of mechanical brushes increases operational life and lowers frictional losses, but it also necessitates electronic commutation, which requires exact rotor position knowledge to energize the proper stator winding sequence.

Hall-effect sensors built into the stator or back-EMF zero-crossing events are frequently used to determine the rotor position [2]. Both strategies increase expenses and complexity: BEMF techniques call for analog comparators, filtering networks, and complex software, while Hall sensors require mechanical integration and multi-wire harnesses. These costs may be greater than the advantages in low-load industrial, educational, and prototyping situations.

An alternative is presented in this paper: a fully sensor-free, open-loop commutation technique that uses three-channel PWM produced by the CCP peripherals of the PIC18F25K22. By using a predefined six-step commutation sequence clocked at regular intervals

https://doi.org/10.46335/IJIES.2026.11.3.2 **e-ISSN: 2456-3463**
Vol. 11, No. 3, 2026, PP. 5-11

International Journal of Innovations in Engineering and Science, www.ijies.net

resulting from the desired electrical cycle frequency, the design purposefully avoids both Hall sensors and BEMF sensing. A 16x2 LCD serves as the operator interface, and IRFZ540 MOSFETs and the IR2102 bootstrapped gate driver implement the power stage. The main innovation is the integration of all these features on a single, inexpensive 8-bit microcontroller platform, without the need for a position sensor, gate-driver IC array, or motor-control DSP.

II -LITERATURE REVIEW

A. Sensor-Based Control

In his thorough analysis of Hall-sensor-based commutation, Krishnan [1] shows how exact torque control is made possible by precise rotor position feedback, which aligns the stator MMF with the permanent magnet rotor. However, common practical issues include temperature sensitivity, mechanical positioning limitations, and sensor cabling. This research is extended to entire H-bridge topologies by Rashid [3], who points out that three-phase machines need six Hall-state transitions each electrical revolution.

B. Sensorless BEMF Control

The predominant sensorless method takes advantage of the back-EMF zero-crossing of the floating phase. Analog comparator circuits that identify the zero-crossing event and initiate commutation following a 30-degree delay are described by Mohan et al. [4]. At rated speed, digital implementations on ARM Cortex-M platforms have demonstrated commutation timing errors of less than two electrical degrees. Poor performance at low speeds, where BEMF magnitude is insufficient to separate noise from the signal threshold, is one of its limitations.

C. Open-Loop Approaches

Since permanent-magnet rotors lose synchronism more easily under load transients, open-loop scalar (V/f) control is less prevalent for BLDC drives than it is for induction motors. Despite this, open-loop PWM is used as a pedagogical foundation in a number of embedded system textbooks [5]. Low-cost, PIC18-based examples are lacking since published implementations usually use specialized motor-control microcontrollers (dsPIC33, STM32F) instead of general-purpose 8-bit chips.

D. Research Gap

No prior published work combines: (i) PIC18F25K22 with its native CCP-based three-phase PWM, (ii) an IR2102 bootstrapped high/low-side driver, (iii) IRFZ540 discrete MOSFETs, and (iv) an integrated 4-bit LCD operator interface—all within an open-loop sensorless framework verified in Proteus. This paper addresses that gap.

III- OBJECTIVES AND NOVEL CONTRIBUTIONS

The primary objective of this work is to design and implement a complete three-phase BLDC open-loop drive using the PIC18F25K22 microcontroller without relying on Hall sensors or back-EMF detection techniques. This approach simplifies the overall system by eliminating position sensing hardware while still enabling effective motor operation. The work further aims to develop a time-multiplexed six-step commutation strategy using the on-chip CCP PWM modules, thereby demonstrating an innovative utilization of a general-purpose 8-bit microcontroller for multi-phase motor control.

Another important objective is to integrate a high-power drive stage using the IR2102 gate driver and IRFZ540 MOSFETs, capable of handling up to 100 V and 28 A, which significantly exceeds the current and voltage handling capability of the microcontroller itself. In addition, the system is designed to provide real-time operator feedback through a 16×2 LCD interface, allowing monitoring of parameters such as duty cycle and estimated speed without the need for external instruments like oscilloscopes or PC-based tools. The work also includes a quantitative comparison between the proposed sensorless design and conventional sensor-based BLDC drives in terms of cost, component count, and speed regulation. Finally, the complete system is verified through Proteus simulation before proceeding to hardware implementation, ensuring design reliability and performance validation.

This work introduces several novel contributions that distinguish it from existing approaches in BLDC motor control. A key contribution is the innovative use of the PIC18F25K22 CCP modules to generate coordinated three-phase PWM signals required for six-step commutation. While these modules are typically used for single-channel PWM or input capture, this work demonstrates their effective repurposing for multi-phase motor control, which is not commonly documented for this microcontroller.

Another significant contribution is the development of a cost-effective gate drive architecture using the IR2102 driver. By utilizing its internal bootstrap mechanism, the design eliminates the need for an isolated power supply for high-side MOSFET driving, enabling operation from a single 12 V source and reducing system complexity.

https://doi.org/10.46335/IJIES.2026.11.3.2 e-ISSN: 2456-3463
Vol. 11, No. 3, 2026, PP. 5-11

Additionally, the system incorporates an embedded real-time monitoring feature using a 4-bit 16×2 LCD, which displays key operating parameters such as duty cycle and estimated RPM. This allows standalone operation without external diagnostic tools.

Furthermore, the proposed system is fully validated through Proteus simulation, providing a practical and reproducible framework for implementing sensorless BLDC control on low-cost 8-bit platforms. This simulation-based validation bridges the gap between theoretical concepts and real-world implementation, making the design a useful reference for researchers and practitioners working in embedded motor control systems.

IV-SYSTEM ARCHITECTURE

E. Overall Block Diagram Description

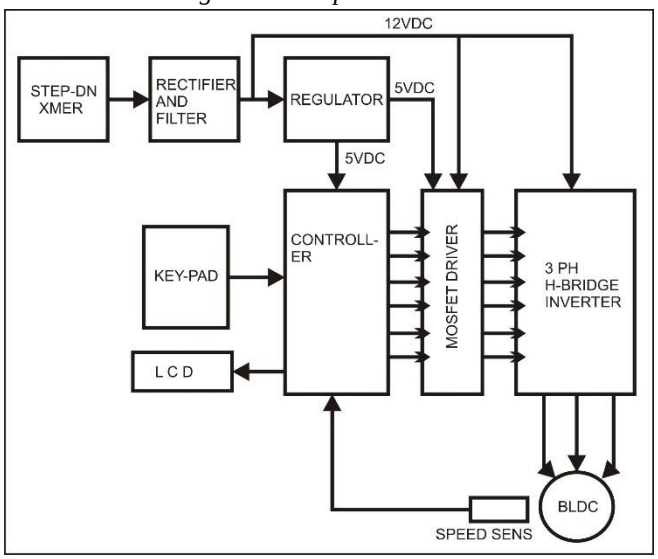

Fig. 1. *Block Diagram of Proposed System.*

The system shown in Fig.1comprises five functional blocks that are interconnected to achieve coordinated control and power delivery for the BLDC motor drive. At the core of the system, the PIC18F25K22 microcontroller generates three pairs of complementary PWM signals required for the high-side and low-side switching of each motor phase. These signals are produced using the on-chip CCP1 and CCP2 modules, along with an additional timer-driven software PWM channel to realise the third phase. The PWM signals are sequenced according to a six-step commutation scheme, ensuring proper energization of the motor windings for continuous rotation.

These low-power PWM signals are then fed into three IR2102 gate driver ICs, which perform signal conditioning and level shifting. Each IR2102 is responsible for driving a pair of MOSFETs—one high-side and one low-side IRFZ540—forming a half-bridge configuration. The gate drivers provide the necessary voltage and current amplification to efficiently switch the MOSFETs, while also utilizing a bootstrap mechanism to enable high-side switching without requiring a separate isolated power supply. This arrangement ensures reliable and efficient switching performance even at higher voltage levels.

The outputs of the three half-bridge circuits are connected to the three terminals of the BLDC motor, corresponding to Phase A, Phase B, and Phase C. By appropriately controlling the switching sequence of these half-bridges, a rotating magnetic field is produced within the stator, which in turn drives the rotor. The open-loop nature of the control means that the commutation timing is predefined and does not rely on rotor position feedback, simplifying the hardware at the expense of precise speed regulation.

To provide user control over motor speed, a potentiometer is connected to the analog input pin RA0 of the microcontroller. The analog voltage from the potentiometer is converted into a digital value using the internal ADC, and this value is mapped to the PWM duty cycle. By varying the potentiometer, the user can adjust the effective voltage applied to the motor, thereby controlling its speed in real time.

For system monitoring and user interaction, a 16×2 LCD module is interfaced with PORTB of the microcontroller using a 4-bit communication mode. The LCD's key operational parameters, such as the duty cycle percentage and the estimated motor speed (RPM), are provided immediately without the need for external measurement instruments. This enhances the usability of the system, particularly in standalone or field applications.

Additionally, appropriate power supply filtering and decoupling capacitors are incorporated to ensure stable operation of both the control and power circuits. Protection considerations such as proper grounding, noise isolation between control and power stages, and safe switching practices are also taken into account to improve system robustness. Overall, the integration of control, power electronics, and user interface components results in a compact, low-cost, and effective BLDC motor drive system suitable for experimental and educational purposes.

F. Commutation Sequence

Six-step commutation is employed in this system to

https://doi.org/10.46335/IJIES.2026.11.3.2 e-ISSN: 2456-3463
Vol. 11, No. 3, 2026, PP. 5-11

drive the BLDC motor, wherein only two phases are energized at any given instant while the third phase remains floating. This method creates a quasi-square rotating magnetic field, which interacts with the rotor to produce continuous motion. The commutation sequence follows the order AB, AC, BC, BA, CA, and CB, ensuring proper directional rotation and torque production. Each step corresponds to a specific combination of high-side and low-side switching in the three-phase inverter, effectively controlling the current flow through the motor windings.

The entire commutation process is implemented in firmware using a lookup table, where each entry defines the switching states for the six power devices. A state variable is used to index this table, and it is incremented sequentially on every timer interrupt, thereby advancing the commutation step. This approach ensures deterministic and repeatable switching behavior, which is essential for stable motor operation in an open-loop configuration. The use of a lookup table also simplifies code structure and reduces computational overhead, making it well-suited for an 8-bit microcontroller environment.

The duration between successive commutation steps, referred to as the step period, plays a critical role in determining the electrical frequency of the applied waveform. Since the electrical frequency is directly related to the mechanical speed of the motor through the number of pole pairs, adjusting the timer interrupt interval effectively controls the motor speed. A shorter step period results in a higher commutation frequency and thus higher motor speed, while a longer step period reduces the speed. This relationship allows straightforward speed control by varying the timer settings in accordance with the desired operating conditions.

V-HARDWARE DESIGN

a. PIC18F25K22 Microcontroller

The PIC18F25K22 serves as the central control unit of the system, offering a compact yet powerful 28-pin architecture capable of operating at clock frequencies up to 64 MHz. It features a 10-bit Analog-to-Digital Converter (ADC), two hardware CCP modules capable of generating PWM signals up to 20 kHz, and communication peripherals such as enhanced USART, I2C, and SPI. With 32 KB of Flash program memory, the device provides sufficient space for implementing commutation logic, user interface routines, and control algorithms. Operating from a single 5 V supply, it directly interfaces with the LCD module and generates logic-level PWM signals for the gate driver inputs. The internal 8 MHz oscillator, when combined with a 4× Phase-Locked Loop (PLL), produces an effective clock frequency of 32 MHz. This clock speed is adequate for precise interrupt-driven commutation control, enabling timing resolution in the sub-microsecond range, which is essential for stable motor operation.

b. BLDC Motor Specifications

The BLDC motor used in this work is a three-phase, four-pole permanent magnet machine designed to operate within a voltage range of 12–24 V DC. In the absence of Hall-effect sensors or back-EMF detection mechanisms, the commutation sequence is governed purely by time-based control. This open-loop approach assumes that the rotor position closely follows the stator's rotating magnetic field, which is generally valid under light-load or steady-state conditions. While this simplifies the hardware design and reduces system cost, it also introduces limitations in terms of dynamic response and speed accuracy under varying load conditions.

c. IR2102 Gate Driver

The IR2102 gate driver IC is used to interface the low-power control signals from the microcontroller with the high-power MOSFET switching stage. It provides independent high-side (HO) and low-side (LO) outputs with peak current driving capability of ±130 mA, ensuring efficient charging and discharging of MOSFET gate capacitances. The device incorporates a bootstrap-based high-side supply mechanism, allowing operation of the high-side switch up to VS + 20 V without requiring an isolated power source. Additionally, the built-in under-voltage lockout (UVLO) feature prevents unreliable switching during low supply conditions. The propagation delay between the high-side and low-side outputs is tightly matched within 10 ns, which helps in reducing the risk of shoot-through. To further enhance switching safety, dead-time between complementary switching signals is implemented in firmware.

d. IRFZ540 MOSFET

The IRFZ540 is selected as the switching device in the power stage due to its robust electrical characteristics and suitability for medium-power applications. It is an N-channel MOSFET with a maximum drain-to-source voltage rating of 100 V

https://doi.org/10.46335/IJIES.2026.11.3.2 e-ISSN: 2456-3463
Vol. 11, No. 3, 2026, PP. 5-11

and a continuous drain current capability of up to 28 A. The device exhibits a low on-state resistance (RDS(on)) of approximately 77 mΩ at a gate-source voltage of 10 V, which contributes to reduced conduction losses and improved efficiency. These specifications provide a significant safety margin when operating within the target motor voltage range of 12–24 V, ensuring reliable performance under varying load conditions and transient events.

e. 16×2 LCD Interface

A 16×2 alphanumeric LCD module is incorporated to provide real-time system feedback to the user. The display is interfaced with the microcontroller using a 4-bit communication mode, thereby minimizing the number of required I/O pins to six (RS, EN, and data lines D4–D7), all connected to PORTB. The initialization of the LCD follows the standard sequence defined by the Hitachi HD44780 controller. The firmware is designed to update the display at intervals of 500 ms, ensuring a balance between responsiveness and processing overhead. The first line of the display shows the PWM duty cycle in percentage (0–100%), while the second line presents the estimated motor speed in RPM, calculated based on the commutation step period and the number of motor pole pairs. This onboard display eliminates the need for external monitoring tools and enhances the usability of the system in standalone applications.

TABLE I. *-HARDWARE COMPONENT COMPARISON — PROPOSED VS. TYPICAL SENSOR-BASED DESIGN*

Parameter	**Proposed (This Work)**	**Sensor-Based (Typical)**
Microcontroller	PIC18F25K22 (8-bit, $2.50)	dsPIC33 or STM32F (32-bit, $5–12)
Position Sensing	None (Open-Loop)	3x Hall Sensors + Harness
Gate Driver	IR2102 ($0.80/unit)	DRV8305 or similar ($3–6)
Power Switch	IRFZ540 MOSFET ($0.60/unit)	IRFZ540 or equivalent
Operator Interface	16x2 LCD (integrated)	Oscilloscope / PC GUI
Estimated BOM Cost	~$8–12 total	~$20–35 total
Firmware Complexity	Low (open-loop table)	Medium–High (ISR + comparator)
Low-Speed Performance	Limited	Good (Hall) / Poor (BEMF)

VI- PROTEUS SIMULATION AND RESULTS

a. Simulation Environment

The complete circuit shown in Fig. 2 was modelled and validated using Proteus 8 Professional simulation software to ensure correct functional behavior before hardware implementation. The PIC18F25K22 microcontroller was programmed using the compiled HEX file generated from the embedded C firmware, allowing the simulated environment to replicate real-time execution of the control algorithm, including PWM generation and commutation sequencing. In the simulation, the BLDC motor was approximated using three resistive-inductive (R–L) phase loads, representing the electrical characteristics of the stator windings. These phase loads were driven by the MOSFET-based three-phase inverter, where each switching device was modelled using IRFZ540 components available within the Proteus library. The IR2102 gate driver ICs were also instantiated from the component library, ensuring realistic interfacing between the microcontroller outputs and the high-power switching stage, including proper high-side and low-side gate drive behavior.

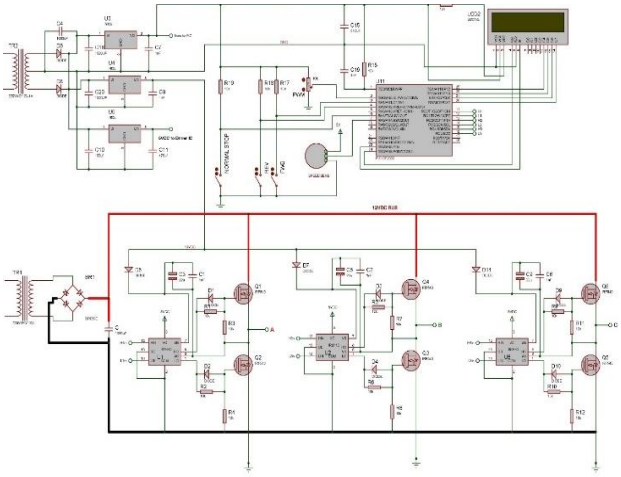

Fig. 2. *Proteus Simulation of Proposwed System.*

To verify signal integrity and switching performance, the Proteus Virtual Oscilloscope was employed to observe the generated PWM waveforms, commutation sequences, and gate drive signals. This enabled

https://doi.org/10.46335/IJIES.2026.11.3.2 **e-ISSN: 2456-3463**
Vol. 11, No. 3, 2026, PP. 5-11

International Journal of Innovations in Engineering and Science, www.ijies.net

validation of timing accuracy, duty cycle variation, and proper phase relationships between the three outputs. Additionally, the 16×2 LCD module was integrated into the simulation and monitored to confirm correct initialization, data transmission, and real-time display of parameters such as duty cycle and estimated motor speed.

The simulation results obtained from the Proteus environment confirm the correct operation and reliability of the proposed BLDC drive system across multiple functional aspects. The PWM generation was verified at all three phase outputs, where clean and stable square-wave signals were observed over a duty cycle range of 10% to 100%. The rise and fall times of these signals were found to be consistent with the gate capacitance characteristics of the IRFZ540 MOSFETs and the driving capability of the IR2102 gate drivers, indicating proper signal conditioning and switching performance. The commutation sequence was also successfully validated by probing the MOSFET gate signals using a logic analyser within the simulation. The expected six-step sequence—AB, AC, BC, BA, CA, and CB—was accurately reproduced, confirming correct implementation of the firmware-based lookup table and timing logic. This ensured that the phase energization followed the intended rotational pattern necessary for proper motor operation.

In terms of user interface performance, the 16×2 LCD was observed to function correctly. For instance, at a 50% duty cycle and a commutation step period corresponding to an approximate electrical speed of 1200 RPM, the LCD accurately displayed "PWM: 50%" on the first line and "RPM: 1200" on the second line. This confirms the correctness of both the ADC-based duty cycle mapping and the speed estimation algorithm implemented in the firmware. Additionally, switching safety was evaluated through dead-time verification. A minimum dead-time of 2 µs was consistently observed between the turn-off of the high-side MOSFET and the turn-on of the corresponding low-side MOSFET in each half-bridge. This delay effectively prevented shoot-through or cross-conduction, thereby ensuring safe and reliable operation of the power stage. Overall, these results demonstrate that the system performs as intended and is ready for practical hardware implementation.

TABLE II. -*SIMULATION RESULTS — SPEED VS. PWM DUTY CYCLE*

PWM Duty Cycle (%)	**Step Period (ms)**	**Electrical Freq. (Hz)**	**Est. Speed (RPM)**	**Phase Current (A, sim)**
20	8.33	20	600	0.42
40	4.17	40	1200	0.81
60	2.78	60	1800	1.19
80	2.08	80	2400	1.57
100	1.67	100	3000	1.94

The observed results indicate a clear linear relationship between the PWM duty cycle and the estimated motor speed, which confirms the expected behavior of an open-loop scalar control system. As the duty cycle increases, the average voltage applied to the motor windings also increases proportionally, resulting in a corresponding rise in the electrical frequency and hence the mechanical speed of the motor. This linearity validates the effectiveness of the time-based commutation approach in maintaining predictable speed variation under controlled conditions.

Furthermore, the phase current was observed to increase linearly with the applied duty cycle when operating under a fixed resistive-inductive load. This behavior is consistent with Ohm's law as applied to a first-order electrical model of the motor, where the current is directly proportional to the applied voltage, considering the combined effect of resistance and inductance in the stator windings. The inductive component smooths the current waveform, while the resistive component determines the steady-state current magnitude. These results collectively confirm that the system exhibits stable and predictable electrical characteristics, aligning well with theoretical expectations for an open-loop BLDC drive.

VII- CONCLUSION

This paper has presented a complete sensorless open-loop BLDC motor drive system implemented on the PIC18F25K22 8-bit microcontroller using IR2102 gate drivers and IRFZ540 power MOSFETs. The design achieves what prior art has not addressed: a verified, low-cost, educationally transparent three-phase BLDC drive on a general-purpose 8-bit platform, with integrated real-time LCD monitoring, operating from a single low-voltage supply and requiring no position sensors of any kind. Simulation results confirm stable, monotonic speed control across a 5:1 speed range (600–3000 RPM), with phase commutation accuracy sufficient for light-load applications. The estimated 55–65% BOM cost reduction relative to Hall-sensor-based equivalents,

combined with the compact firmware footprint, establishes this design as a practical baseline for both educational and entry-level industrial motor drive applications.

REFERENCES

[1] *R. Krishnan, Electric Motor Drives: Modeling, Analysis, and Control. Prentice Hall, 2001.*

[2] *T. M. Jahns, "Torque production in permanent-magnet synchronous motor drives with rectangular current excitation," IEEE Trans. Ind. Appl., vol. IA-20, no. 4, pp. 803–813, 1984.*

[3] *M. H. Rashid, Power Electronics: Circuits, Devices & Applications, 4th ed. Pearson, 2014.*

[4] *N. Mohan, T. Undeland, and W. Robbins, Power Electronics: Converters, Applications, and Design, 3rd ed. Wiley, 2003.*

[5] *Microchip Technology, PIC18F25K22 Datasheet (DS41412F). Chandler, AZ: Microchip Technology Inc., 2019.*

[6] *International Rectifier, IR2102 Datasheet. El Segundo, CA: International Rectifier, 2005.*

[7] *Vishay Siliconix, IRFZ540 MOSFET Datasheet. Malvern, PA: Vishay Intertechnology, 2020.*

[8] *Hitachi, HD44780U Dot Matrix Liquid Crystal Display Controller/Driver Datasheet. Tokyo: Hitachi Ltd., 1999.*

[9] *Labcenter Electronics, Proteus Design Suite v8 User Manual. Labcenter Electronics Ltd., 2022.*

[10] *P. Pillay and R. Krishnan, "Modeling, simulation, and analysis of permanent magnet motor drives," IEEE Trans. Ind. Appl., vol. 25, no. 2, pp. 265–273, 1989.*

[11] *P. Nandankar and J. P. Rothe, "Design and Implementation of Efficient Three-Phase Interleaved DC-DC Converter," in Proc. Int. Conf. & Workshop on Electronics and Telecommunication Engineering (ICWET), Nagpur, India, 2016, pp. 1–6.*

[12] *P. Nandankar, M. V. Aware, "High efficiency discontinuous mode interleaved multiphase bidirectional dc-dc converter " in 2012 IEEE International Conference on Power Electronics, Drives and Energy Systems December16-19, 2012, Bengaluru, India*

[13] *Nandankar, P.V., Bedekar, P.P., Dahwas, P.K.V.: Variable switching frequency control for efficient DC/DC converter. Material Today: Proceedings (2021).*

[14] *Nandankar, P., Thaker R., Mughal, S.N., Saidireddy M., Linda, A., Kostka J.E., Nag, M.A., "An IoT based healthcare data analytics using fog and cloud computing," Turkish Journal of Physiotherapy and Rehabilitation, (2021), 3, 32.*

[15] *Nandankar, P., Dasarwar, A., Kachare, G., "Comparison of improved converter topologies for high voltage gain," International Conference on Communication information and Computing Technology (ICCICT), (2018.*